The Molecular Mechanism of DNA Polymerases Studied by Small-Angle X-Ray Scattering (SAXS)

Kuo-Hsiang Tang[1], William T. Heller[2], Gary W. Lynn[2], and Ming-Daw Tsai[1]

[1] Department of Chemistry and Biochemistry, the Ohio State University, Columbus, OH 43210, USA.

[2] Chemical Sciences Division and Center for Structural Molecular Biology, Oak Ridge National Laboratory, Oak Ridge, TN 37831, USA

ABSTRACT

DNA replication is a fundamental biological process required for cellular reproduction. The central feature of DNA replication is the template-induced nucleotidyl transfer reaction mediated by DNA polymerases. Critical to this function is the maintenance of high fidelity (accuracy) in the insertion of dNTP in the event of polymerases-mediated elongation of the primer. The structure-function relationship of DNA polymerases has been an active subject of research for decades. It is widely accepted that the high fidelity of dNTP insertion is controlled by closure of the DNA polymerases dNTP-binding subdomain in response to binding the appropriate dNTP. The model also holds that no such conformational change occurs in response to the incorrect dNTPs. This is the so-called "induced-fit" mechanism. However, no structural information in support of the model exists for mismatched ternary complexes. Additionally, most of the structural information about the functional mechanism of DNA polymerases resulted from crystallographic studies, and very few or no solution structural studies have been reported on various DNA polymerases and their E-DNA complexes. Here we present solution small-angle X-ray scattering (SAXS) structural studies on two DNA polymerases, mammalian DNA polymerase β (Pol β) and DNA polymerase X (Pol X) from African sworn fever virus (ASFV). In response to binding DNA, the Pol β-DNA (E-DNA) binary complex adopts a more compact conformation than free E. In the addition of dNTP onto E-DNA binary complex, the complex undergoes a further compaction, possibly suggesting closure of dNTP binding domain by incorporating dNTP, but the nucleotidyl specificity for the conformational change was not observed. Such changes are consistent with previous crystallographic studies on Pol β. In the reaction of Pol X, in which lacks DNA binding domain in its native form, no structures have been reported for either the binary or the ternary complex. However, previous biochemical studies on Pol X have suggested that binding of DNA is not weaker even though the DNA-binding subdomain is not present on Pol X. Our SAXS studies suggest that that a very different conformation exists for the binary complex compared to the free E and ternary complex based on the analyses of their Dmax, Rg, and peak position of P(r). In summary, our preliminary studies have shown that SAXS is a feasible approach for obtaining structural information about the molecular mechanism of Pol β and Pol X.

INTRODUCTION

Conformational changes on DNA polymerases have been detected by crystallographic studies.

a. *b.*

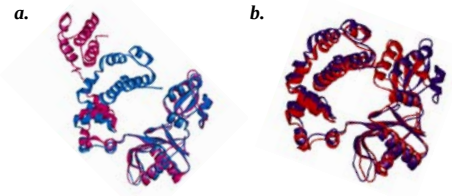

Figure 1. Comparisons between different crystal structures of Pol β. Superimposition of the free form (**1BPD**, shown in pink) v.s. the binary complex (**1BPX**, only protein part of structures is shown in cyan) of Pol β (a). Superimposition of the binary (**1BPX**, shown in purple) v.s. the ternary (**1BPY**, shown in red) complex of Pol β (b). These crystal structures have suggested that in response to binding DNA, the Pol β-DNA (E-DNA) binary complex adopts a more compact conformation than free E. The binary complex undergoes a further compaction upon (corrected) dNTP insertion.

RESULTS from SAXS Studies

Pol β

a

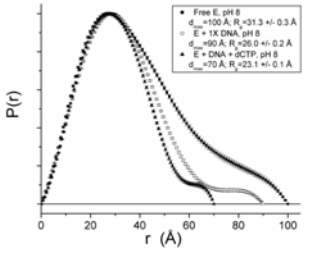

-More compact structure was suggested from SAXS measurements in response of DNA binding onto the free E and incorporations of dNTP onto the binary complex.

b

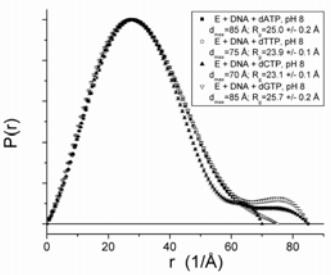

- Subtle differences were obtained from the addition of pyrimidine base (to form G:C (matched) and G:T) versus the addition of purine base (to form G:A and G:G) onto the binary complex of Pol β.

Figure 2. Plots of P(r) curve for Pol β and its complexes (a) and for the addition of dNTP onto the binary complex of Pol β (b).

Pol X

a

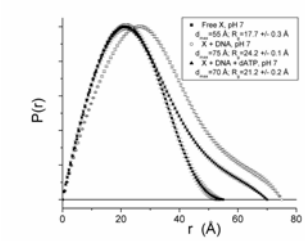

-Very different peak positions on P(r) plots and larger Rg for the binary complex versus the free form and the addition of dNTP onto the binary complex of Pol X were suggested by the SAXS measurements.

b

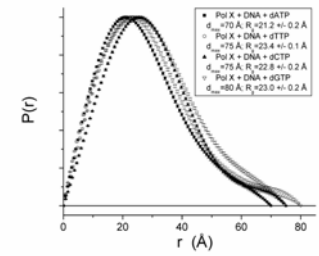

-More Differences on P(r) plots were observed in the addition of various dNTPs onto binary complex of Pol X versus onto that of Pol β (Figure 2b).

Figure 3. Plots of P(r) curve for Pol X and its complexes (*a*) and for the addition of dNTP onto the binary complex of Pol X (*b*).

Table 1: Results for radii of gyration (Rg) of Pol β and its complexes.

Component \ Rg (Å)	Rg (Guinier)	Rg (GNOM)	Rg (Crysol, predicted from crystallographic structures)
Free E	30.0 +/- 0.8	31.3 +/- 0.3	27.8 (1BPD)
Binary complex	25.1 +/- 0.1	25.6 +/- 0.1	23.7 (1BPX) 24.3 (1BPE)
Ternary complexes (the addition of various dNTP onto the binary complex)			
G (template) : A (primer)	24.9 +/- 0.2	25.0 +/- 0.2	
G (template) : T (primer)	24.3 +/- 0.3	23.9 +/- 0.1	
G (template) : C (primer) (matched base pairing)	23.8 +/- 0.2	23.1 +/- 0.1	22.8 (1BPY)
G (template) : G (primer)	25.8 +/- 0.2	25.7 +/- 0.2	

Table 2: Results for radii of gyration (Rg) of Pol X and its complexes.

Component \ Rg (Å)	Rg (Guinier)	Rg (GNOM)	Rg (Crysol, predicted from NMR structures)
Free E (reduced form)	17.7 +/- 0.5	17.7 +/- 0.3	17.53 (1JAJ) 17.46 (1JQR)
Binary complex	25.0 +/- 0.3	24.2 +/- 0.1	
Ternary complexes (the addition of various dNTP onto the binary complex)			
G (template) : A (primer)	20.9 +/- 0.3	21.2 +/- 0.2	
G (template) : T (primer)	23.9 +/- 0.3	23.4 +/- 0.1	
G (template) : C (primer) (matched base pairing)	23.3 +/- 0.3	22.8 +/- 0.2	
G (template) : G (primer)	22.2 +/- 0.3	23.0 +/- 0.2	19.8 (predicted from ref. 7)

Qualitative 2D-^{15}N-HSQC NMR studies: Very different HSQC NMR spectra were obtained for binary and ternary complexes of Pol X, and global conformational differences were not suggested by NMR studies on dNTPs insertions onto the binary complex of Pol X.

a *b*

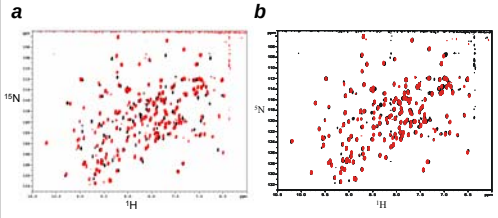

Figure 4. Superimposition of 2D-15N-HSQC NMR spectra of the binary (black) and ternary (G:G, red) complexes of Pol X (*a*) and of mismatched G:A (black) and G:G (red) ternary complexes (*b*).

METHODS

SAMPLE PREPARATION-- DNA Polymerases used in the studies were expressed and purified as described previously (*1*, *2*). The DNA substrate used for SAXS measurements of E + ddD_n(binary) and E + ddD_n + dNTP (ternary) complexes was a 16/10(dd)/5 gapped DNA with the sequence: 3'-GCTGATGCGCCGTCGG-5' (template) paired with 5'-GCTGATGCG(ddC)-3' (10(dd) primer) and 5'-(phosphate)-GTCGG-3' (downstream primer). The ddD_n stands for the DNA substrate with dideoxynucleotide terminated (ddC) primer, which prevents the proceeding of the chemical step, such that the stable complexes of (E•ddD_n•dNTP) ternary complexes can be formed in the solution. The sequence of DNA substrate used herein is the same as applied previously for crystallographic studies of Pol β (*3*, *4*) and NMR studies of Pol X (*2*).

SAMPLES FOR ANALYSES -- For scattering experiments on free E form of Pol β and Pol X, 0.2 mM Pol β or Pol X was mixed with 10 mM of Mg2+, 10 mM DTT, 50 mM phosphate buffer (at pH 7.0 or 8.0), and 0.15 M (for Pol β) or 0.5 M (for Pol X) K+ at 20 oC. 0.2 mM of ddDNA and additional 10 mM dNTP was added to the above solution to study the conformation of binary and ternary complexes of Pol β/Pol X, respectively.

DATA COLLECTION-- SAXS experiments were conducted on synchrotron beamline 4-2 at Stanford Synchrotron Radiation Laboratory (SSRL). Data were collected at a wavelength of 1.3776 Å and sample to detector distance of 1.5 m with the sample maintained at a constant temperature of 20 °C. The initial beam flux was 2 x 10^{10} photons/sec/cm^2 and scattered X-rays were collected using a linear gas chamber detector (200mm x 4mm active area), whose detector channel numbers were converted to Q (the momentum transfer) using the reflection of cholesteryl myristate. The sample cell (15 µL volume) is constructed from polycarbonate and includes flat mica windows. Scattering was monitored in 10-min exposure times for the sample. Repeated measurements of the same sample yield the same results, indicating that no significant radiation damage occurred during the experiments. The buffer background scattering was subtracted from the sample scattering.

DATA ANALYSES--For a dilute, monodisperse solution of homogenous particles, the intensity $I(q)$ is related to the radius of gyration (Rg) of a single particle by the Guinier law (*5*):

$$\ln(I(q)) = \ln(I(0)) - \frac{(qR_g)^2}{3} \qquad \text{(Equation 1)}$$

The molecular weight of the particle is calculated from the value of $I(0)$, thus giving evidence as to the presence or absence of aggregation, which manifests as an upturn in the low-q data, or artifacts due to interparticle interference, which manifest as a decreased $I(0)$, in the experimental sample. Rg is a shape-independent geometric function (second moment) and defines the average distance from the center of a particle to scattering segments within that particle. The Guinier law may be used for any particle of unknown size or shape; however, there are instances when it is not valid. In order to use Guinier analysis three conditions must be satisfied: (i) the system is rotationally isotropic, (ii) the particles in the system scatter independently of each other, (iii) $q*Rg < 1.3$ which is explicit to the Guinier law.

Additional analysis can be performed to provide more information on the shape of the scattering particle. It is convenient to invert Equation 2, thereby generating the distance distribution function $P(r)$ from the experimental $I(q)$ curve using the Fourier transform in Equation 2.

$$P(r) = \frac{1}{2\pi^2}\int_0^\infty dq \cdot (qr) \cdot I(q) \cdot \sin(qr) \qquad \text{(Equation 2)}$$

The program GNOM (*6*) was used to determine $P(r)$ from the measured scattering intensity $I(q)$. $P(r)$ is the distribution of interparticle vector lengths within a single scattering particle. From $P(r)$, it is possible to determine $dmax$, the maximum linear dimension of the particle.

Working Hypothesis and Summary

A. Our SAXS measurements on Pol β (Figure 2a) are consistent with previous crystallographic studies on Pol β (Figure 1), except that the nucleotidyl specificity for the conformational change was not observed (Figure 2*b*).

B. The binary complex of Pol X has very different conformation compared to their free form and ternary complexes. Based on its larger Dmax and Rg from SAXS measurements and peak changes on 2D HSQC NMR spectra, it is possible that the binary complex of Pol b can be a functional dimer, which may lead to tight DNA binding of Pol X, where the DNA-binding subdomain is not present.

C. The differences on Rg, dmax and P(r) plots by SAXS studies for dNTP insertions onto binary complex of Pol X can be rationalized as (1) the ternary complexes of Pol X has very different ternary complexes, where NMR studies suggested otherwise, or as (2) the equilibrium between the binary and ternary complexes led to the differences on SAXS profiles (two-population model, see below).

D. Two-population (equilibrium) model: The SAXS data for various ternary complexes of Pol β and Pol X are resulting from the ensemble of binary and ternary complexes. While mismatched dNTP is incorporated onto the binary complex, their less favorable interactions led to larger Rg because of more binary complex (less compact structure) population in the reaction. Their ternary complexes, however, might be quite similar based on the qualitatively NMR studies (Figure 4). In contrast to qualitative HSQC NMR studies, SAXS studies herein are more sensitive to detect the mix states for incorporations of dNTPs onto binary complexes of Pol X.

-- SAXS data resulting from an ensemble of structures can be difficult to identify, depending on the nature of the differences between the states. The conformational states of the binary and ternary complexes of Pol X are very distinct, so the mixed states can be easily seen from P(r) plots (**Figure 3**). In contrast, the conformations of the binary and ternary of Pol β don't vary dramatically in SAXS studies, so the changes on P(r) plots are more subtle (**Figure 2**).

REFERENCES

[1] Werneburg, B.G., Ahn, J., Zhong, X., Hondal, R.J., Kraynov, V.S., and Tsai, M.-D. (1996) Pre-steady-state kinetic analysis and the roles of arginine-283 in catalysis and fidelity. *Biochemistry* **35**, 7041-7050.

[2] Showalter, A.K., Byeon, I.J., Su, M.I., and Tsai, M.-D. (2001) Solution structure of a viral DNA polymerase X and evidence for a mutagenic function. *Nat. Struct. Biol.* **8**, 942-6.

[3] Sawaya, M.R, Prasad, R., Wilson, S.H, Kraut, J., and Pelletier, H (1997) Crystal structures of human DNA polymerase β complexed with gapped and nicked DNA: evidence for an induced fit mechanism. *Biochemistry* **36**, 11205-11215.

[4] Pelletier, H., Sawaya, M.R., Wolfle, W., Wilson, S.H., and Kraut, J. (1996) Crystal structures of human DNA polymerase β complexed with DNA: Implications for catalytic mechanism, processivity, and fidelity. *Biochemistry* **35**, 12742-12761.

[5] Guinier, A., and Fournet, G. (1955) *Small-Angle Scattering of X-Rays*, John Wiley & Sons, Inc.

[6] Svergun, D. I. (1992) Determination of the regularization parameter in indirect-transform methods using perceptual criteria *J. Appl. Crystallogr.* **25**, 495-503.

[7] Sue, M.-I., Tang, K.-H., and Tsai, M.-D. Manuscipt in preparation.

Acknowledgements: Portions of this research were carried out at the Stanford Synchrotron Radiation Laboratory, a national user facility operated by Stanford University on behalf of the U.S. Department of Energy, Office of Basic Energy Sciences. The SSRL Structural Molecular Biology Program is supported by the Department of Energy, Office of Biological and Environmental Research, and by the National Institutes of Health, National Center for Research Resources, Biomedical Technology Program.